Journal of Theoretical and Applied Information Technology

31st October 2023. Vol.101. No 20

ISSN: 1992-8645 www.jatit.org E-ISSN: 1817-3195

MDCGANOCIS: MODIFIED DEEP CONVOLUTIONAL GENERATIVE ADVERSARIAL NETWORKS BASED ORAL CANCER IDENTIFICATION SYSTEM

DHARANI R[1] , REVATHY S[2] , DANESH K[3] , PEERTHI PARAMESWARI[4] , AISHWARYA B[5]

[1]Associate Professor, Panimalar Engineering College, Department. of IT, Tamilnadu, India
[2]Associate Professor, Sathyabama Institute of Science and Technology, School of Computing, Tamil Nadu, India
[3]Assistant Professor, SRMIST, Department of ECE, Ramapuram Campus, Tamilnadu, Inida.
[4,5]Assistant Professor, SRMIST, Department of IT, Ramapuram Campus, Tamilnadu, Inida.

Email : [1]dharanir.pec@gmail.com, [2]ramesh.revathy@gmail.com, [3]danesh.kn1@gmail.com
[4]preethiparameswari8@gmail.com, [5]aishwarb@srmist.edu.in

ABSTRACT

This paper develops a novel feature extraction model based on Generative Adversarial Networks (GAN) and Convolution Neural Network (CNN) to detect the oral cancer with high accuracy. The main objective of this work is to classify the input Oral Cavity Squamous Cell Carcinoma (OCSCC) image as healthy or sick. The methods used here are, Modified Deep Convolution Generative Adversarial Networks (MDCGAN) as feature extractor and Modified Convolution Neural Network (MCNN) is used for classification oral cancer images. Before extracting process, the first step is to image enhancement. For this step, first input image is resized, contrast enhanced and finally RGB color space is converted into YCbCr color space. For contrast enhancement in this work uses the Improved CLAHE method. The study found that proposed work gives best result than existing approaches. Performance of the proposed technique in terms of classification precision during the testing phase. The suggested method achieving impressive accuracy, precision, recall, and f1-score rates of 97.83%, 97.50%, 95.12%, and 96.30%, respectively, for magnification 400x, and 98.11% accuracy for magnification 100x. during the testing phase. The originality of this work is in the application of the MDCGAN feature extraction model, which is based on deep learning, to obtain pertinent features for classification. The overall quantity and caliber of the features extrapolated from the OCSCC image determine how well oral cancer will be predicted. The accuracy will grow if feature sizes are expanded. GAN is typically used to increase the dataset's image count. However, in our method, deep feature extraction is done via GAN. The generator components of our suggested MDCGAN model operate similarly to conventional GAN. This section is used to increase the dataset's sample size for each image. The accuracy will grow if feature sizes are expanded. However, MCNN replaces the discriminator component of traditional GAN. The detection precision for oral cancer prediction will increase with the use of this innovative MDCGAN feature model. Therefore, MDCGAN is far superior to conventional deep learning algorithms for such image classification applications.
Keywords: *Oral Cancer, Deep Learning, Classifiers, Real-Time, CNN, MDCGAN, DCGAN*

1. INTRODUCTION

Oral squamous cell carcinomas (OSCC) account for more than 90% of all oral cancers, a heterogeneous group of tumors that develop from the mucosal lining of the oral cavity [1, 2]. Oral squamous cell carcinoma (OSCC) is the sixth most prevalent subtype of head and neck squamous cell carcinoma (HNSCC) on a global basis [4]. An estimated 657,000 new cases are diagnosed each year, resulting in a severe mortality rate of more than 330,000. It is worth noting that oral squamous

cell carcinoma (OSCC) is particularly prevalent in South Asian countries. India had the most cases, accounting for over one-third of the total, despite Pakistan having the greatest prevalence of malignancies in both men and women,

ranking second overall [5]. Alcohol consumption, smoking, poor oral hygiene, HPV exposure, genetic predisposition, lifestyle choices, ethnicity, and geographical location are all risk factors for oral squamous cell carcinoma (OSCC). The earliest detection of oral squamous cell carcinoma (OSCC) is critical in order to properly execute treatment options, slow the disease's progression, and reduce death and hospitalization rates [6]. Nonetheless, the general prognosis for oral squamous cell carcinoma (OSCC) remains poor, as evidenced by a 50% cure rate [7, 8]. The fundamental method for identifying oral squamous cell carcinoma (OSCC) is to examine clinical specimens histologically under a microscope [9, 10]. However, this process can be time-consuming and error-prone, limiting the efficacy of diagnostic pathology methods [11]. As a result, providing clinicians with appropriate diagnostic tools for the evaluation and detection of oral squamous cell carcinoma (OSCC) is critical. There have been noteworthy advances in the field of study relevant to the use of artificial intelligence (AI) for the goal of supplementing clinical tests in recent years. The increased use of diagnostic imaging has allowed researchers to study the possible applications of artificial intelligence (AI) in the processing of healthcare pictures. Deep learning (DL) has proven to be particularly effective in addressing a variety of challenges linked with healthcare image processing, such as aberrant picture detection [14, 15]. On a wide scale, computer-aided diagnostic (CAD) techniques have showed successful development and deployment in a variety of cancer types, including breast, lung, and prostate cancer [16-18].

The current body of literature on the use of deep learning (DL) in the diagnosis of oral cancer has been demonstrated to be limited in breadth. Nonetheless, numerous studies have had hopeful results. Dev et al., for example, used Convolutional Neural Network (CNN) and Random Forest algorithms to detect keratin pearls in oral histology images. Their research yielded classification rates of 96.88% and 98.05%, respectively, using CNN and Random Forest techniques [19]. Similarly, Das et al. used deep learning (DL) algorithms to classify oral biopsy pictures using Broder's histological grading system. Their convolutional neural network (CNN) implementation achieved a significant classification accuracy of 97.5% [20]. Folmsbee et al. found that Active Learning (AL) performed better than Random Learning (RL) by 3.26% in a separate study. This was especially evident when Convolutional Neural Networks (CNN) were used to categorize oral cancer pictures into seven unique groups [21]. Martino et al. also did research on a variety of deep learning architectures, including U-Net, SegNet, U-Net with VGG16 encoder, and U-Net with ResNet50 encoder. Their study's goal was to categorize oral images into three unique groups: carcinoma, noncarcinoma, and nontissue. In comparison to the regular U-Net model, the U-Net model with ResNet50 as the encoder performed better [22]. Amin et al. did a study on the binary categorization of images of oral illnesses. The feature extractors and upgraded versions of the Inception V3, VGG16, and ResNet50 networks were used in the study [23]. The aforementioned findings highlight the potential of deep learning (DL) in the diagnosis of oral cancer. Various models have shown promising results in a variety of image processing tasks. The combined deep learning approach utilizing Modified Deep Convolutional Generative Adversarial Network (MDCGAN) and Modified Deep Convolutional Neural Network (MDCNN), aims to enhance the efficiency of oral cancer detection during both training and testing stages. The main contributions of this novel approach are mentioned here:

- ***Image Enhancement:*** The proposed approach includes a process of image enhancement using resizing and contrast enhancement with the Improved CLAHE method to prepare the input images for better analysis.
- ***Novel Feature Extraction Model:*** This paper introduces a Modified Deep Convolutional Generative Adversarial Network (MDCGAN) for feature extraction, which can improve the accuracy of oral cancer prediction.
- ***MCNN Classification:*** The traditional Discriminator in GAN is replaced with a Modified Convolutional Neural Network (MCNN) for feature discrimination, aiding in accurate classification of oral cancer images.

2. RELATED WORK

Oral cancer is a significant global health challenge, and researchers have been actively exploring the potential of artificial intelligence

(AI) and machine learning to aid in its detection and diagnosis. Du et al. [1] conducted a study on the incidence trends of lip, oral cavity, and pharyngeal cancers based on global burden data from 1990 to 2017, providing valuable insights into the disease's epidemiology. Li et al. [2] focused on the role of circ_LPAR3 in the progression of OSCC, contributing to the understanding of cancer pathogenesis. In the context of head and neck cancer, Perdomo et al. [4] explored the burden in Central and South America and discussed preventive measures, while Anwar et al. [5] investigated clinic pathological features and risk factors in a high-risk population in Pakistan. Chakraborty et al. [6] presented a review of advances in oral cancer detection, showcasing the importance of technological developments in improving diagnostic accuracy. Moreover, Eckert et al. [7] shed light on the HIF-1-dependent metabolism in oral squamous cell carcinoma, providing insights into tumor behavior and potential therapeutic targets. AI and machine learning have played a crucial role in oral cancer risk prediction, as demonstrated by Ghosh et al. [8], who proposed a deep reinforced neural network model for automated risk assessment based on cyto-spectroscopic analysis. While the field of oral cancer detection has been significantly impacted by AI, similar advancements have been observed in other areas of cancer research.

Deif and Hammam [9] applied deep learning techniques for skin lesions classification, highlighting the broader applicability of AI in medical image analysis. Similarly, Kong et al. [10] used computer-aided evaluation for neuroblastoma on whole-slide histology images, demonstrating the potential of AI in various cancer types. In the context of diagnostic accuracy, Santana and Ferreira [11] discussed diagnostic errors in surgical pathology, emphasizing the importance of technological support to minimize discrepancies. Moreover, AI has shown promise in predicting outcomes and treatment efficacy, as observed in Deif et al. [14], where a hybrid XGBoost-AHP approach was used for an automated triage system during the COVID-19 pandemic. AI has ushered in a new era of clinical biomarkers, as seen in Echle et al.'s work [15], where deep learning was utilized for cancer pathology, including oral cancer. Additionally, Duggento et al. [16] focused on deep computational pathology in breast cancer, further exemplifying AI's potential as a clinical tool. Wang et al. [17] and Goldenberg et al. [18] showcased AI's application in lung cancer and prostate cancer, respectively, demonstrating its versatility across different cancer types. In the realm of oral cancer specifically, Das et al. [19] worked on the automatic identification of clinically relevant regions in oral tissue histological images for oral squamous cell carcinoma diagnosis. Furthermore, Das et al. [20] employed transfer learning and convolutional neural networks for the automated classification of cells in oral squamous cell carcinoma epithelial tissue, showcasing the utility of deep learning models in this domain.

Folmsbee et al. [21] emphasized the importance of active deep learning in improving training efficiency for tissue classification in oral cavity cancer. Martino et al. [22] utilized deep learning-based pixel-wise lesion segmentation on oral squamous cell carcinoma images, highlighting the potential for automated segmentation and analysis. Amin et al. [23] presented a concatenated deep learning model for histopathological image analysis, further demonstrating AI's potential for oral squamous cell carcinoma classification. Finally, recent studies have explored AI in oral cancer risk prediction. Alhazmi et al. [26] investigated the application of AI and machine learning for predicting oral cancer risk, while Chu et al. [27] focused on treatment outcome prediction in oral cancer. Welikala et al. [28] proposed an automated detection and classification system for oral lesions using deep learning, emphasizing the potential for early oral cancer detection. In conclusion, the literature survey reveals a wealth of research on AI's application in oral cancer detection and diagnosis. From epidemiological studies to advanced deep learning models, AI continues to pave the way for improved detection, risk prediction, and treatment outcomes in oral cancer.

3. METHODOLOGY

The architecture presented in Figure 1 is designed for discovering and detecting oral cancer using both offline and online techniques. During the offline training phase, a dataset of cancer tissue images is collected, annotated with cancer-affected and healthy regions, and pre-processed for further analysis. To learn features and distinguish between cancerous and healthy tissues, a deep learning model called MDCGAN is employed. Additionally, a MCNN is trained to

ISSN: 1992-8645 www.jatit.org E-ISSN: 1817-3195

classify whether an image is healthy or not. In the online testing phase, in which real-time oral images are fed into the system, they are sourced from various places, including patients' oral cavity images. These images undergo essential pre-processing steps, such as resizing, contrast enhancement, and color space conversion, to ensure they are in an appropriate format for further analysis. Subsequently, the system extracts relevant features from the pre-processed images using feature extraction techniques, which play a crucial role in detecting cancer-affected regions. By identifying potential cancerous areas within the oral images, the derived features are then fed into the trained MCNN model to detect whether the patient is affected by cancer or not. This integrated approach aims to enhance the accuracy and efficiency of oral cancer detection.

The proposed DCGANOCIS-based oral cancer detection model is structured into three main stages: (i) image pre-processing, (ii) feature extraction using MDCGAN, and (iii) MCNN-based oral cancer prediction. Further details regarding each of these phases are elaborated in the following subsections.

3.1 Pre-Processing

This section presents the details of the pre-processing steps applied to prepare oral cancer images for subsequent feature extraction model and identification in oral cancer. The pre-processing include image resizing, contrast enhancement, and color space conversion. These steps are crucial in standardizing the images and enhancing their quality, ultimately facilitating the accuracy and effectiveness of the cancer identification process.

3.1.1 Image resizing

In the first step of the pre-processing, the input oral cavity cancer image is resized from its original size (1665×1393×3) to a new size of 227x227x3. This process is commonly referred to as image resizing. Resizing the image ensures that it is in a standardized format, making it suitable for further analysis and feature extraction in the subsequent stages of the oral cancer detection process.

3.1.2 Contrast enhancement

The Improved Contrast Limited Adaptive Histogram Equalization (I- CLAHE) algorithm is a technique used to enhance the contrast of an image. The process begins by loading a scaled picture, which could have been resized before enhancement. The green component of the image undergoes Discrete Wavelet Transform (DWT) to extract its frequency information. Subsequently, the Inverse Discrete Wavelet Transform (IDWT) is applied to reconstruct the enhanced green component. To further improve the contrast, the CLAHE technique is employed on the blue component of the image. I-CLAHE enhances the local contrast while limiting over-amplification of noise. Finally, the original red component, the newly enhanced green component, and the improved blue component are combined to create an upgraded RGB image with enhanced contrast and improved visual quality. Algorithm for improved CLAHE is in Table 1.

Table 1. Algorithm for improved CLAHE

Algorithm: *Improved CLAHE*
Input: *Resized image*
Output: *Enhanced RGB image*
Steps:
1. Apply DWT to the green component
2. Reconstruct enhanced green component
3. Apply CLAHE to the blue component
4. Combine the RGB components to create the upgraded RGB image

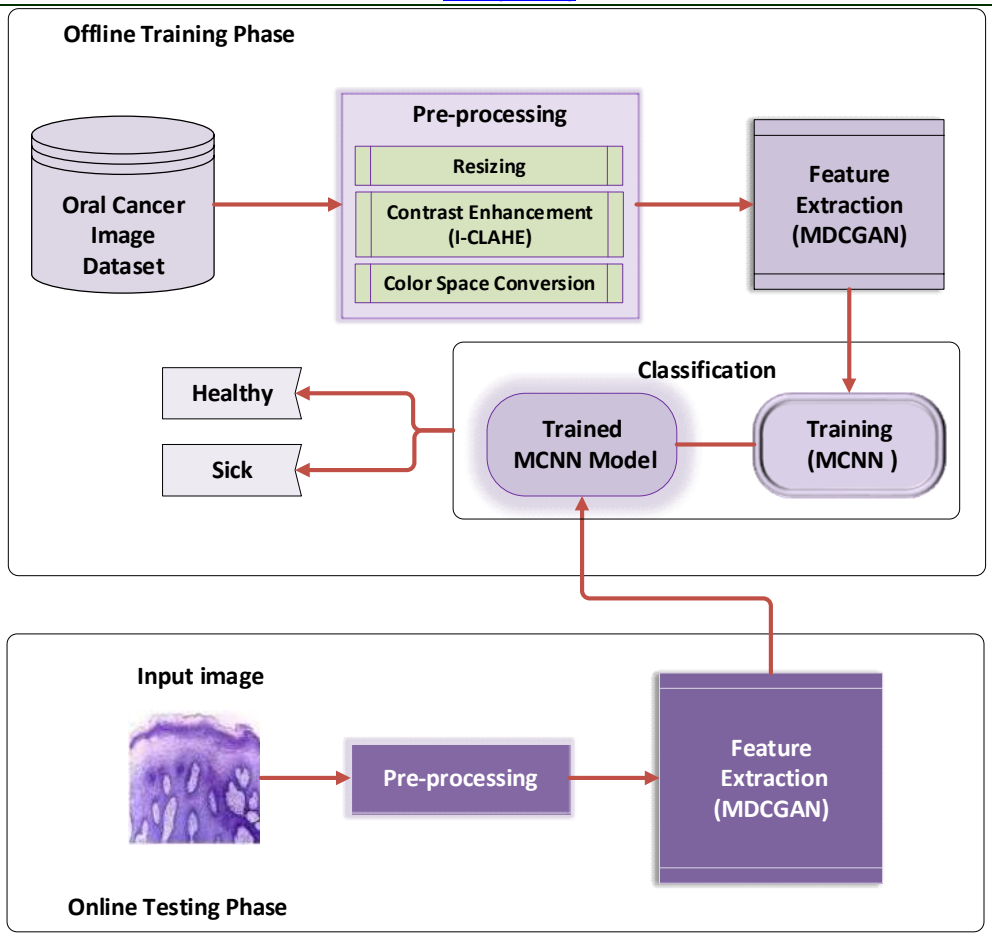

Figure 1. Overall architecture of proposed DCGANOCIS model

3.1.3 Color space conversion

In computer graphics and digital imaging, the commonly used color space is the red, green, and blue (RGB) color space. It represents color using three primary hues - red, green, and blue - with each component ranging from 0 to 255. However, the RGB color space has some limitations, especially when dealing with changes in lighting conditions. To address these challenges, the YCbCr color space is derived from the RGB color space. The YCbCr color space separates color information from luminance information. The conversion equations transform RGB values into YCbCr values. The luminance component (Y) represents brightness, while the chrominance components $(Cb\ and\ Cr)$ represent color difference information.

$$Y = 0.412453 * R + 0.357580 * G + 0.180423 * B \quad (1)$$
$$Cb = 0.21267 * R + 0.715160 * G + 0.072169 * B \quad (2)$$
$$Cr = 0.019334 * R + 0.119193 * G + 0.950227 * B \quad (3)$$

This color space can provide color and illumination robustness, efficient representation, and capture discriminative color information.

3.2 Feature Extraction Model

The feature extraction model transforms pre-processed data into informative representations, leading to improved performance in oral cancer diagnosis. Figure 2 illustrates the architecture of the proposed MDCGAN model.

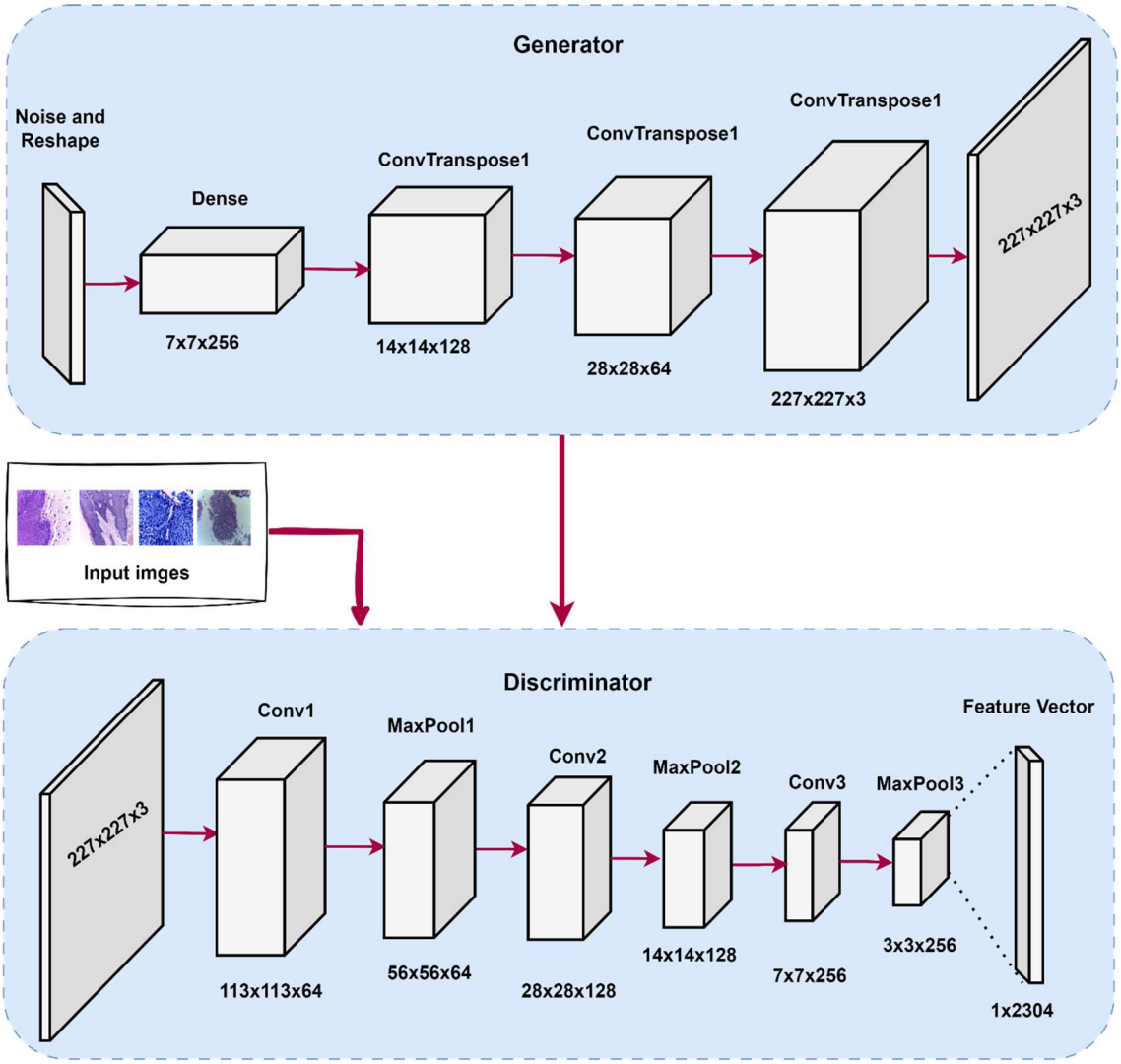

Figure 2. Architecture of proposed MDCGAN model

3.2.1 Modified Deep Convolutional Generative Adversarial Network

Deep Convolutional Generative Adversarial Network (DCGAN) is a novel feature extraction model that leverages the strengths of both GAN and CNN for feature extraction from pre-processed images. In MDCGAN, the discriminator in a standard GAN is replaced with a MCNN. This modification for the model to explicitly focus on feature extraction rather than image generation. The generator network takes random noise as input and uses fractional stride convolutions up sample the noise into a feature map. Batch normalization and relu, activations are applied to improve stability and introduce non-linearity. It utilizes minimax adversarial training, where the generator aims to create synthetic feature map that can deceive the discriminator into misclassifying it as real, while the discriminator aims to accurately distinguish between real and synthetic data. The mathematical formulation is defined as:

$$F^{D} = E_{a\sim p_a}\left[log\ log\ D(a)\right] + E_{z\sim p_z}\left[log\ log\left(1 - D(G(z))\right)\right] \quad (4)$$

$$F_G = E_{z\sim p_z}\left[log\ log\left(1 - D(G(z))\right)\right] \quad (5)$$

Where, p_a is the a distribution, p_z is the z distribution, $D(a)$ is the possibility for real distribution, $G(z)$ is the generated sample, F_D *and* F_G are the discriminator and generator objective function respectively, and E is the

expectation, Layer configurations of generator is shown in Table 2.

Table 2. Layer configurations of generator in MDCGAN model

Layer	Input Size	Output Size	Number of Filters	Kernel Size	Stride
Input Noise	**100**	-	-	-	-
Dense	**100**	**7x7x256**	**256**	-	-
ConvTranspose1	**7x7x256**	**14x14x128**	**128**	**5x5**	**2**
ConvTranspose2	**14x14x128**	**28x28x64**	**64**	**5x5**	**2**
ConvTranspose3	**28x28x64**	**227x227x3**	**3**	**7x7**	**4**
Output (Tanh)	**227x227x3**	**227x227x3**	-	-	-

In proposed MDCGAN, MCNN act as the discriminator, which has learned to distinguish between real and fake images, is utilized as a feature extraction module. By passing generator output to the discriminator layers up to a certain intermediate point before the final classification layer, meaningful features are extracted. These extracted features can then be used for oral cancer prediction. Table 3 presents the configurations of the layers employed in the discriminator model

Table 3. Layer configurations of discriminator in MDCGAN model

Layer	Input Size	Output Size	Number of Filters	Kernel Size	Stride
Input Image	**227x227x3**	-	-	-	-
Conv1	**227x227x3**	**113x113x64**	**64**	**3x3**	**2**
MaxPool1	**113x113x64**	**56x56x64**	-	**2x2**	**2**
Conv2	**56x56x64**	**28x28x128**	**128**	**3x3**	**2**
MaxPool2	**28x28x128**	**14x14x128**	-	**2x2**	**2**
Conv3	**14x14x128**	**7x7x256**	**256**	**3x3**	**2**
MaxPool3	**7x7x256**	**3x3x256**	-	**2x2**	**2**
Flatten	**3x3x256**	**2304**	-	-	-
Output (Feature Vector)	**1x2304**	**1**	-	-	-

3.3 Classification using MCNN

After feature extraction, the 1x1024 feature map is reshaped into a 32x32 matrix to be used for classification using the MCNN architecture, which is the customized version of the traditional CNN architecture specifically designed to improve performance for an oral cancer detection. The modifications in MCNN involves the expansion of the network architecture with the addition of more convolutional layers. This strategic augmentation deepens the hierarchy of feature representations within the model, enabling it to learn more intricate and abstract features. The initial layers of the MCNN capture fundamental low-level features such as edges, textures, and color gradients, while the subsequent deeper layers progressively learn higher-level features that encapsulate more complex and informative patterns. This hierarchical learning allows the model to recognize the complex spatial relationships and nuanced structures present in oral cancer images, thus facilitating better detection accuracy. These deep layers enable the model to recognize complex patterns associated with oral cancer, leading to better detection accuracy. Figure 3 illustrates the architecture of the proposed MCNN model.

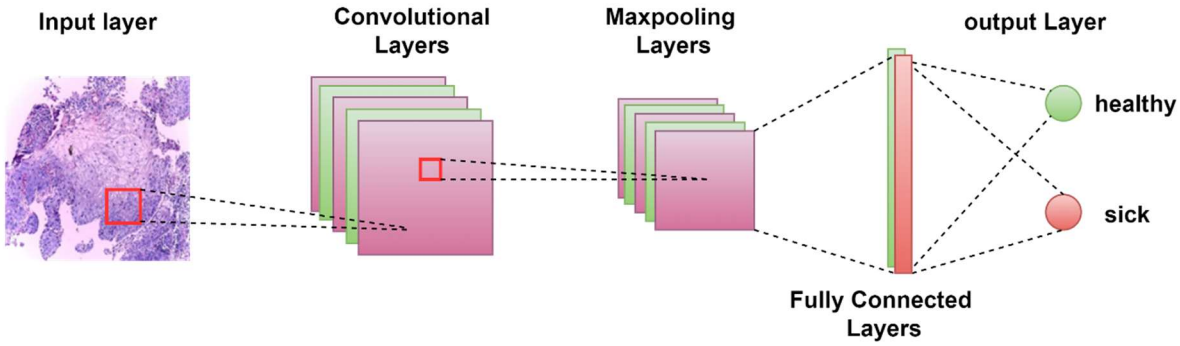

Figure 3. Architecture of proposed MCNN model

Convolutional layer: The convolutional layer is a fundamental building block of CNN that plays a crucial role in detecting patterns and features within input image. Comprising learnable channels or neurons with small receptive fields, the layer performs convolutions with filters over the input, generating feature maps that capture spatially specific information. By adapting its parameters during training, the CNN learns to recognize increasingly complex features, enabling it to efficiently extract relevant information and reduce data redundancy. The convolution process is defined as,

$$C_j^i = F\left(\sum_{x\in R_c}^{\mathrm{n}} \mathrm{b}\, C_x^{i-1} * \omega_j^i + b_j^i\right) \quad (6)$$

where, C_j^i denotes the output of the i^{th} kernel in the convolutional layer j, R_c is the convolution region, ω_j^i is the weight in convolutional layer in, b_j^i denotes the bias vector, and $F(*)$ is a nonlinear activation function.

Pooling layer: Following the convolutional layer, the CNN employs a max pool layer, which serves to reduce dimensions and extract essential feature information from the previous output. By selecting the maximum value within small regions, this layer effectively retains the most significant features while discarding less relevant details, aiding in preventing overfitting. In this architecture, the combination of convolutional and max pool layers creates a powerful feature extraction process, enabling the network to learn and generalize complex patterns efficiently, making it robust for classification. The pooling operation is defined as,

$$C_j^i = F\left(\omega_j^i * max\left(C_j^{i-1}\right) + b_j^i\right) \quad (7)$$

where $max(*)$ represents the max pooling function, C_j^i is the output of the pooling layer.

Fully Connected layer: The final step in a CNN involves using a fully connected layer to map the extracted feature information into the classifier. This process includes flattening the feature maps, performing a weighted sum with learnable weights and biases, applying an activation function for non-linearity, and obtaining the output for prediction. Mathematically the process is explained as,

$$O^k = F(\omega^k C^{k-1} + b^k) \quad (8)$$

Where, O^k is the output for the final connected layer and k is the network.

Loss function: The binary cross-entropy loss function applies stronger penalties to the model's confident incorrect predictions, thereby encouraging the network to improve its predicted probabilities towards the true labels during training. The objective in classification tasks is to minimize the binary cross-entropy loss as it enables effective training of MCNN. The loss function is in eqn. 9.

$$L_f = -\frac{1}{N} * \sum_{n=1}^{N} \mathrm{n}\, y_n * log\ log\ (nw(I_n)) + (1 - y_n) * log\ log\ (1 - nw(I_n)) \quad (9)$$

Where, N is the number of total samples used for training, y_n be the true label of the sample n, I_n be the input for training sample n, and nw represents the neural network weights. Layer configurations of the proposed MCNN model in Table 4.

Table 4. Layer configurations of the proposed MCNN model

Layer	Input Size	Output Size	Number of Filters	Kernel Size	Stride
Input Image	**48x48x1**	-	-	-	-
Conv1	**48x48x1**	**48x48x32**	**32**	**3x3**	**1**
ReLU1	**48x48x32**	**48x48x32**	-	-	-
MaxPool1	**48x48x32**	**24x24x32**	-	**2x2**	**2**
Conv2	**24x24x32**	**24x24x64**	**64**	**3x3**	**1**
ReLU2	**24x24x64**	**24x24x64**	-	-	-
MaxPool2	**24x24x64**	**12x12x64**	-	**2x2**	**2**
Conv3	**12x12x64**	**12x12x128**	**128**	**3x3**	**1**
ReLU3	**12x12x128**	**12x12x128**	-	-	-
MaxPool3	**12x12x128**	**6x6x128**	-	**2x2**	**2**
Flatten	**6x6x128**	**4608**	-	-	-
Dense1 (FC1)	**4608**	**512**	**512**	-	-
ReLU4	**512**	**512**	-	-	-
Dense2(FC2)	**512**	**2**	**2**	-	-
Softmax	**2**	**2**	-	-	-

The proposed MCNN architecture consists of three convolutional layers, generating 32, 64, and 128 filters, respectively. These layers effectively detect local patterns and extract intricate features from input images, resulting in feature maps with dimensions of 48x48x32, 24x24x64, and 12x12x128, respectively. Subsequently, three pooling layers with a stride of 2x2 are applied to reduce spatial dimensions, leading to feature maps of 24x24x32, 12x12x64, and 6x6x128. After flattening the output of the last pooling layer, the feature vector becomes a 1D representation of length 4608, which serves as input to the two fully connected layers. The first fully connected layer contains 512 neurons, while the final classification layer has two neurons with a softmax activation function, producing probabilities for the binary classification task. It demonstrates its effectiveness in image classification by using convolutional and pooling layers to capture local and global patterns and extract meaningful features. The softmax activation function refines the predictions, providing probabilities for the two classes, making the MCNN an efficient and reliable system for binary image classification tasks, such as distinguishing between healthy and sick patients in oral cancer classification.

3.4 Proposed DCGANOCIS model

The proposed DCGANOCIS model can be utilized for oral cancer prediction by leveraging the feature extraction capabilities of the MDCGAN to generate oral cancer feature maps. Oral cancer images are then passed through the MDCGAN layers up to an intermediate point, allowing the extraction of meaningful features that capture essential characteristics learned during adversarial training. Subsequently, these extracted features are fed into an MCNN classifier specifically trained for oral cancer prediction. The MCNN classifier learns to associate specific feature patterns with the presence or absence of oral cancer, enabling it to make accurate predictions. The proposed DCGANOCIS model offers a comprehensive and effective solution for oral cancer prediction, and aid in the early detection and diagnosis of oral cancer,

contributing to improved patient outcomes and healthcare interventions. Overall, the proposed model represents a promising advancement in the field of oral cancer prediction, leveraging the power of deep learning and generative adversarial networks to address critical challenges in healthcare.

4. RESULTS AND DISCUSSIONS

In this section, the experimental analysis and comparative results of the proposed DCGANOCIS model are illustrated. The model's performance is evaluated, and a comparison is

made with other relevant methods to assess its effectiveness and capabilities.

This research aim to highlight the unique aspects and potential of our approach in improving the accuracy and efficiency of oral cancer diagnosis.

The limitations and potential conflicting perspectives in the research is

AI in Medical Diagnosis: While AI has shown promise in various medical fields, including image analysis, there are ongoing discussions and debates within the medical community about its role in diagnosis and treatment. Some perspectives emphasize the potential benefits of AI, such as increased efficiency and accuracy, while others raise concerns about overreliance on technology and the importance of human expertise in medical decision-making.

Diagnostic Criteria: The criteria for diagnosing oral cancer, like many other medical conditions, can vary across different medical institutions and regions. It's crucial to acknowledge that our AI models are trained on specific criteria, and variations in diagnostic criteria may impact the model's performance in different settings. Future research should consider standardizing diagnostic criteria to enhance model robustness

Employed a range of performance metrics, including accuracy, sensitivity, specificity, and precision, to evaluate the AI models' effectiveness in oral cancer detection. These metrics are commonly used in medical image analysis to assess diagnostic accuracy and the model's ability to correctly identify cancerous regions

4.1 Experimental Setup

The implementation of the proposed oral cancer prediction method is carried out using MATLAB R2020a on a Windows 10 operating system with 64-bit architecture and 32 GB RAM. This setup offers an efficient and straightforward approach to execute the method effectively.

4.2 Data Description

The dataset used in this study is publicly available Dataset [29], which consists of two magnifications, each containing images categorized into two groups: healthy and sick. The first set comprises 528 images captured from biopsy slides, with a magnification of 100x. Among these, 89 images represent histopathological samples with normal epithelium of the oral cavity, while the remaining 439 images belong to the Oral Squamous Cell Carcinoma (OSCC) category. Figure 4 presents a selection of images from the OSCC dataset captured at a magnification of 100x.

The second set comprises 696 images captured from biopsy slides, with a magnification of 400x. Among these, 201 images represent histopathological samples with normal epithelium of the oral cavity, while the remaining 495 images belong to the OSCC category. Figure 5 depicts a selection of images from the OSCC dataset captured at a magnification of 400x. Overall dataset description is presented in Table 5.

ISSN: 1992-8645 www.jatit.org E-ISSN: 1817-3195

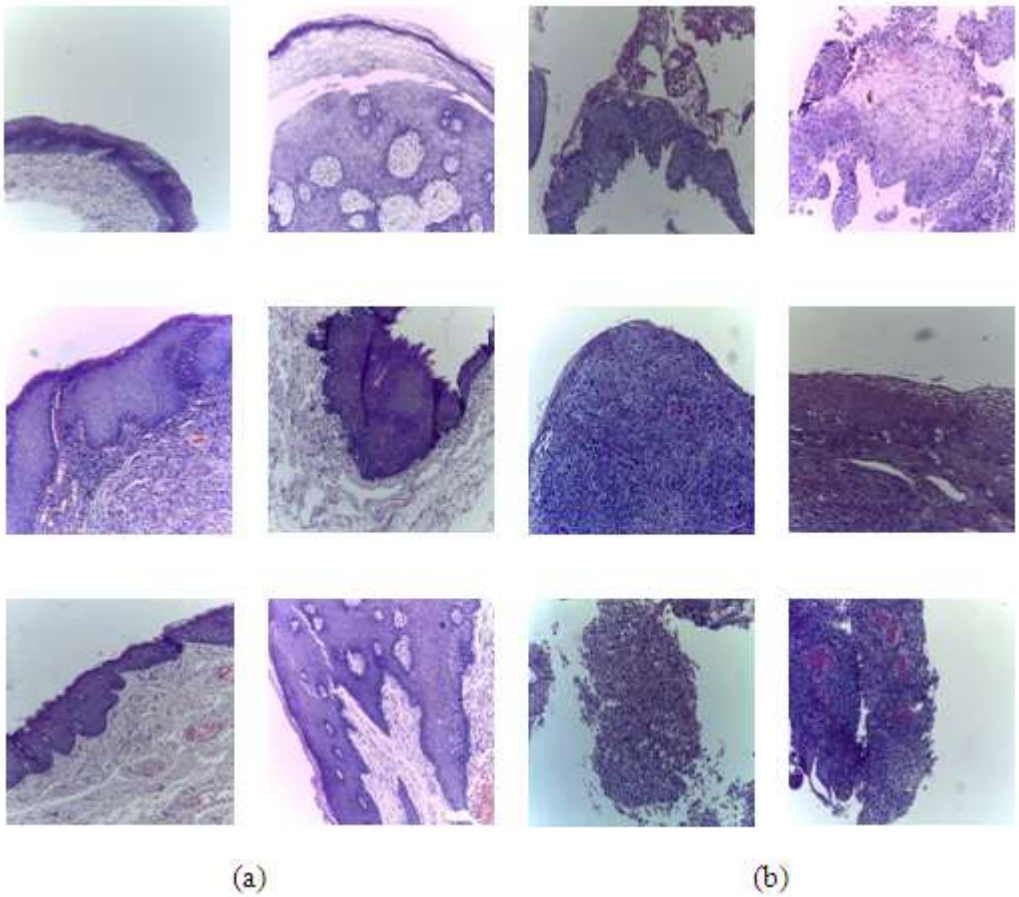

Figure 4. Sample images from OSCC dataset captured at magnification 100x (a) Healthy (b) Sick

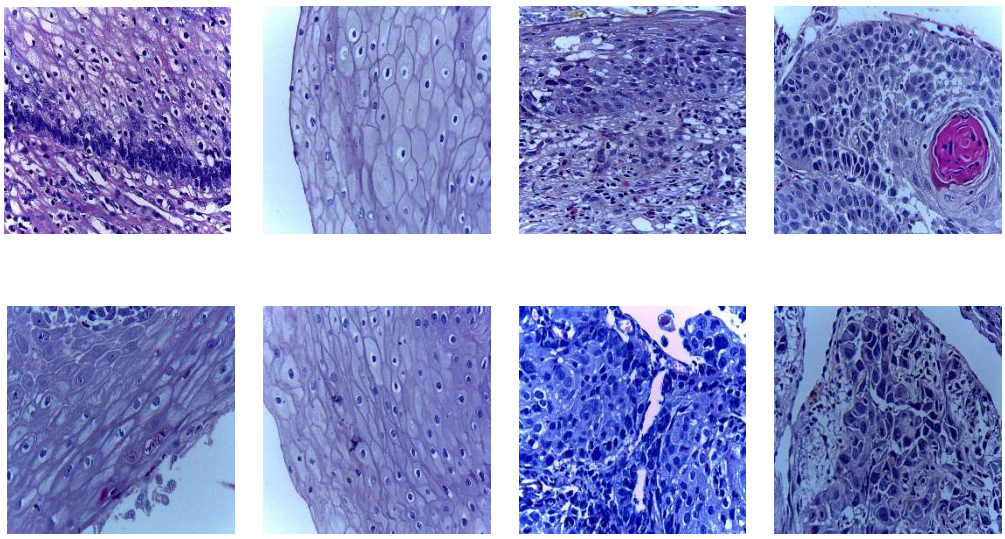

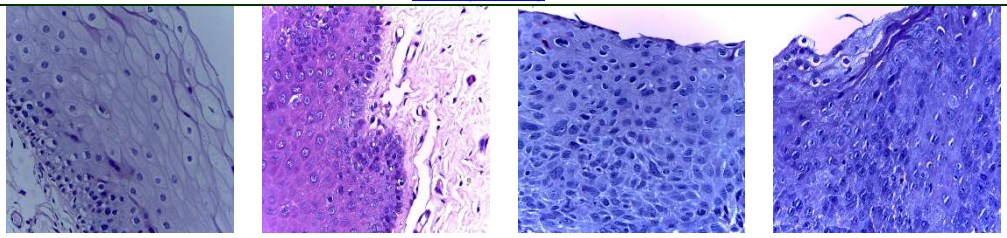

(a) (b)

Figure 5. Sample images from OSCC dataset captured at magnification 400x (a) Healthy (b) Sick

Table 5. Dataset description

Magnification	Classes	Number of Images	Total Images
100x	Sick (OSCC)	495	696
	Healthy	201	
400x	Sick (OSCC)	439	528
	Healthy	89	

4.3 Performance metrics

The evaluation of the prediction algorithms in this work is based on several performance metrics. The paper considers the following evaluation metrics to assess the effectiveness of the proposed model:

Detection Accuracy (DA): The accuracy of the proposed model is evaluated by computing the ratio of true positive, true negative, false positive, and false negative predictions. This equation provides a measure of how well the model correctly identifies both healthy and sick instances in the dataset.

$$DA = \frac{TP+TN}{TP+FP+TN+FN} \quad (10)$$

Precision Rate (PR): The precision rate is the ratio of true positives to all positive predictions made by the model, including both true positives and false positives. It is also known as a high positive predictive value. Precision measures the accuracy of the model's positive predictions and how well it avoids false positive identifications.

$$PR = \frac{TP}{TP+} \quad (11)$$

Recall Rate (RR): It refers to the ratio of true positives in the dataset to the sum of true positives and false negatives. It measures the model's ability to correctly identify positive instances and is particularly relevant when evaluating the model's performance in detecting the target condition.

$$RR = \frac{TP}{TP+FN} \quad (12)$$

F1-Score(F_s): F1 score is the weighted average of precision and recall, providing a balanced evaluation of the model's performance on both positive and negative instances.

$$F_s = 2 * \frac{Precision*Recall}{(Precision*Recall)} \quad (13)$$

4.4 Loss and Accuracy Curve

Figure 6 illustrates accuracy curve of the proposed model for training (80%) and testing (20%). The graph underscores the effectiveness of the model with an impressive 98.11% accuracy, highlighting its high performance. In Figure 7, the loss curve of the proposed model is shown. The loss values indicate that the model achieved its best validation loss value of 0.02 to

0.1 during both the training and testing phases. The model was trained and tested for 100 epochs during the accuracy and loss validation stages. Hyperparameters used for this study is listed in Table 6.

Table 6. Hyperparameters used for classification

Parameters	Values
Loss function	**MAE and MAE**
Optimizer function	**Adam**
Metrics	**Accuracy**
Epochs	**100**
Batch size	**32**
Learning rate	**0.0001**

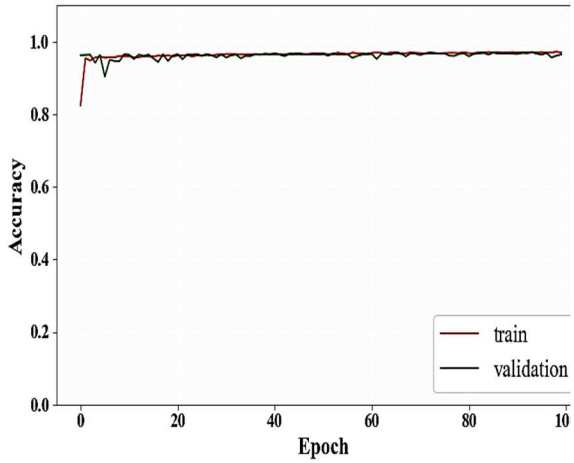

Figure 6. Accuracy curve for the proposed model

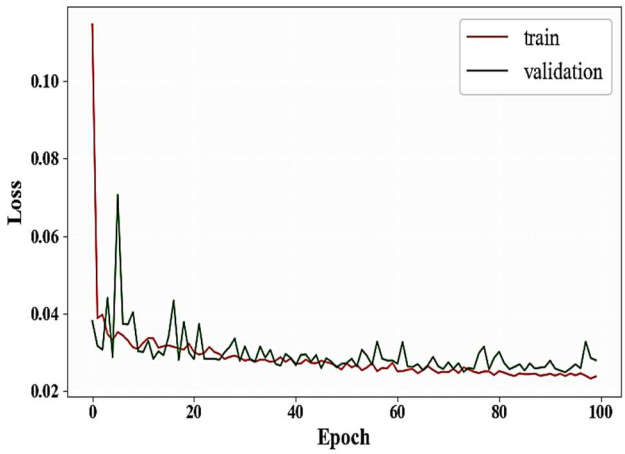

Figure 7. Loss curve for the proposed model

4.5 Comparative Analysis

In this section, the comparative analysis of the proposed DCGANOIS model is deployed for the efficient detection of oral cancer. The methods considered for comparative analysis are KNN [26], ResNet101 [27] and ANN [28]. Table 7 illustrates the partitioning of two OSCC datasets into separate training and testing phases, considering two magnification levels: 400x and 100x. The numbers in parentheses indicate the split ratios used, with 70% and 80% of the samples allocated for training, while the remaining 30% and 20% are designated for testing, respectively.

Table 7. Train-Test Splitting for OSCC Datasets at Different Magnifications

Classes	Magnification: 400x		Magnification: 100x	
	Training (70%)	**Testing (30%)**	**Training (70%)**	**Testing (30%)**
Healthy	62	27	141	60
Sick	307	132	347	148
	Training (80%)	**Testing (20%)**	**Training (80%)**	**Testing (20%)**
Healthy	71	18	161	40
Sick	351	88	396	99

The performance of the proposed DCGANOIS model is thoroughly assessed and compared to three conventional methods: KNN, ResNet101, and ANN. The evaluation is based on the accuracy metric with 80% of the training data for two magnifications, 100x and 400x. For magnification 100x, the conventional methods achieve moderate accuracy values of 87.42%, 91.82%, and 88.68% for KNN, ResNet101, and ANN, respectively. However, the proposed methods, both with and without MDCGAN, exhibit remarkable improvements, achieving significantly higher accuracies of 95.60% and 97.50%, respectively. Similarly, for magnification 400x, the conventional methods achieve accuracies of 88.94%, 93.27%, and 90.87% for KNN, ResNet101, and ANN, respectively. Nevertheless, the proposed methods demonstrate exceptional performances, attaining remarkable accuracies of 96.63% and 97.60%, respectively. For a more comprehensive understanding of the performance metrics, detailed analysis can be presented in Table 8.

Table 8. Comparative analysis based on 70% training and 30% testing data

Methods	**TP**	**FP**	**TN**	**FN**	**Accuracy (%)**	**Precision (%)**	**Recall (%)**	**F1-Score (%)**
Magnification: 100x								
KNN [26]	21	6	14	118	87.42	77.78	60	60.87
ResNet101 [27]	23	4	9	123	91.82	85.19	71.88	77.97
ANN [28]	20	7	11	121	88.68	74.07	64.52	68.97
Proposed without MDCGAN	25	2	5	127	95.60	92.59	83.33	87.72
Proposed with MDCGAN	**26**	**1**	**3**	**130**	**97.50**	**96.30**	**90**	**92.86**
Magnification: 400x								
KNN [26]	49	11	12	136	88.94	81.67	80.33	80.99
ResNet101 [27]	**53**	**7**	**7**	**141**	**93.27**	**88.33**	**88.33**	**88.33**
ANN [28]	51	9	10	138	90.87	85	93.88	84.30
Proposed without MDCGAN	57	3	4	144	96.63	95	93.44	94.21
Proposed with MDCGAN	**58**	**2**	**3**	**145**	**97.60**	**96.67**	**95.08**	**95.87**

The proposed DCGANOIS model's performance is thoroughly evaluated and compared to three conventional methods, namely KNN, ResNet101 and ANN. The evaluation is conducted using the accuracy metric with 80% of the training data for two different magnifications, 100x and 400x. For magnification 100x, the conventional methods achieve moderate accuracy values of 80.19%, 90.57%, and 85.71% for KNN, ResNet101 and ANN, respectively. However, the proposed

methods, both with and without MDCGAN, demonstrate remarkable improvements, achieving significantly higher accuracies of 95.28% and 98.11%, respectively. Likewise, for magnification 400x, the conventional methods are achieving accuracies of 86.33%, 91.30%, and 89.86% for KNN, ResNet101, and ANN, respectively. Nonetheless, the proposed methods, attaining remarkable accuracies of 93.53% and 97.83%, respectively. These findings clearly highlight the superiority of the proposed DCGANOIS model, as it consistently outperforms the conventional methods across both magnification levels. For a more comprehensive understanding of the performance metrics, detailed analysis can be found in Table 9.

Table 9. Comparative analysis based on 80% training and 20% testing data

Methods	TP	FP	TN	FN	Accuracy (%)	Precision (%)	Recall (%)	F1-Score (%)
Magnification: 100x								
KNN [26]	12	6	15	73	80.19	66.67	44.44	53.33
ResNet101 [27]	15	3	7	81	90.57	83.33	68.18	75
ANN [28]	13	5	10	77	85.71	72.22	56.52	63.41
Proposed without MDCGAN	16	2	3	85	95.28	88.89	84.21	86.49
Proposed with MDCGAN	**17**	**1**	**1**	**87**	**98.11**	**94.44**	**94.44**	**94.44**
Magnification: 400x								
KNN [26]	33	7	12	87	86.33	82.50	73.33	77.65
ResNet101 [27]	**36**	**4**	**8**	**90**	**91.30**	**90**	**81.82**	**85.71**
ANN [28]	36	4	10	88	89.86	90	78.26	83.72
Proposed without MDCGAN	37	3	6	93	93.53	92.50	86.05	89.16
Proposed with MDCGAN	**39**	**1**	**2**	**96**	**97.83**	**97.50**	**95.12**	**96.30**

The above analysis indicates that utilizing 80% of the training data in the proposed DCGANOIS model led to superior performance in oral cancer prediction, surpassing the conventional methods' accuracy levels.

The proposed method outperforms existing techniques in terms of performance metrics, mainly due to its effective use of preprocessing techniques that enhance the input data. Additionally, the utilization of MDCGAN feature extraction reduces computational complexity by removing less informative features, further contributing to improved results. As a result, the oral cancer prediction using the proposed DCGANOIS model significantly enhances prediction accuracy through the integration of the MCNN architecture.

5. CONCLUSION

The proposed DCGANOIS model is utilized for disease prediction, demonstrating enhanced efficiency in oral cancer detection using the OSCC dataset. To improve classification accuracy, an improved CLAHE method is employed for data preprocessing. Additionally, the model leverages MDCGAN for feature extraction, feeding the relevant features to the MCNN for classification. Comparative analysis with conventional techniques highlights the model's superiority, achieving impressive accuracy, precision, recall, and f1-score rates of 97.83%, 97.50%, 95.12%, and 96.30%, respectively, for magnification 400x, and 98.11% accuracy for magnification 100x. These results underscore the model's effectiveness in disease prediction, outperforming conventional methods. The study proposes further exploration of additional datasets and advanced algorithms to enhance the classifier's performance, anticipating

continuous advancements in disease prediction and diagnosis with evolving technology in medical research and healthcare.

REFERENCES:

[1] M. Du, R. Nair, L. Jamieson, Z. Liu, and P. Bi, "Incidence trends of lip, oral cavity, and pharyngeal cancers: global burden of disease 1990–2017," Journal of Dental Research, vol. 99, no. 2, pp. 143–151, 2020.

[2] L. Li, Y. Yin, F. Nan, and Z. Ma, "Circ_LPAR3 promotes the progression of oral squamous cell carcinoma (OSCC)," Biochemical and Biophysical Research Communications, vol. 589, pp. 215–222, 2022.

[3] S. Warnakulasuriya and J. S. Greenspan, "Epidemiology of oral and oropharyngeal cancers," in Textbook of Oral CancerSpringer, Berlin, Germany, 2020.

[4] S. Perdomo, G. Martin Roa, P. Brennan, D. Forman, and M. S. Sierra, "Head and neck cancer burden and preventive measures in central and South America," Cancer Epidemiology, vol. 44, pp. S43–S52, 2016.

[5] N. Anwar, S. Pervez, Q. Chundriger, S. Awan, T. Moatter, and T. S. Ali, "Oral cancer: clinicopathological features and associated risk factors in a high-risk population presenting to a major tertiary care center in Pakistan," PloS One, vol. 15, no. 8, Article ID e0236359, 2020.

[6] D. Chakraborty, C. Natarajan, and A. Mukherjee, "Advances in oral cancer detection," Advances in Clinical Chemistry, vol. 91, pp. 181–200, 2019.

[7] A. W. Eckert, M. Kappler, I. GroBe, C. Wickenhauser, and B. Seliger, "Current understanding of the HIF-1-Dependent metabolism in oral squamous cell carcinoma," International Journal of Molecular Sciences, vol. 21, no. 17, 2020.

[8] A. Ghosh, D. Chaudhuri, S. Adhikary, and A. K. Das, "Deep reinforced neural network model for cyto-spectroscopic analysis of epigenetic markers for automated oral cancer risk prediction," Chemometrics and Intelligent Laboratory Systems, vol. 224, Article ID 104548, 2022.

[9] M. A. Deif and R. E. Hammam, "Skin lesions classification based on deep learning approach," Journal of Clinical Engineering, vol. 45, no. 3, pp. 155–161, 2020.

[10] J. Kong, O. Sertel, H. Shimada, K. Boyer, J. Saltz, and M. Gurcan, "Computer-aided evaluation of neuroblastoma on whole-slide histology images: classifying grade of neuroblastic differentiation," Pattern Recognition, vol. 42, no. 6, pp. 1080–1092, 2009.

[11] M. F. Santana and L. C. L. Ferreira, "Diagnostic errors in surgical pathology," JornalBrasileiro de Patologia e Medicina Laboratorial, vol. 53, pp. 124–129, 2017.

[12] M. A. Deif, R. E. Hammam, and A. A. A. Solyman, "Gradient boosting machine based on PSO for prediction of leukemia after a breast cancer diagnosis," International Journal on Advanced Science, Engineering and Information Technology, vol. 11, no. 2, pp. 508–515, 2021.

[13] F. Altaf, S. M. S. Islam, N. Akhtar, and N. K. Janjua, "Going deep in medical image analysis: concepts, methods, challenges, and future directions," IEEE Access, vol. 7, Article ID 99540, 2019.

[14] M. A. Deif, A. A. A. Solyman, M. H. Alsharif, and P. Uthansakul, "Automated triage system for intensive care admissions during the COVID-19 pandemic using hybrid XGBoost-AHP approach," Sensors, vol. 21, no. 19, 2021.

[15] A. Echle, N. T. Rindtorff, T. J. Brinker, T. Luedde, A. T. Pearson, and J. N. Kather, "Deep learning in cancer pathology: a new generation of clinical biomarkers," British Journal of Cancer, vol. 124, no. 4, pp. 686–696, 2021.

[16] A. Duggento, A. Conti, A. Mauriello, M. Guerrisi, and N. Toschi, "Deep computational pathology in breast cancer," Seminars in Cancer Biology, vol. 72, pp. 226–237, 2021.

[17] S. Wang, D. M. Yang, R. Rong et al., "Artificial intelligence in lung cancer pathology image analysis," Cancers, vol. 11, no. 11, p. 1673, 2019.

[18] S. L. Goldenberg, G. Nir, and S. E. Salcudean, "A new era: artificial intelligence and machine learning in prostate cancer," Nature Reviews Urology, vol. 16, no. 7, pp. 391–403, 2019.

[19] D. K. Das, S. Bose, A. K. Maiti, B. Mitra, G. Mukherjee, and P. K. Dutta, "Automatic identification of clinically relevant regions from oral tissue histological images for oral squamous cell carcinoma diagnosis,"

Tissue and Cell, vol. 53, pp. 111–119, 2018.

[20] N. Das, E. Hussain, and L. B. Mahanta, "Automated classification of cells into multiple classes in epithelial tissue of oral squamous cell carcinoma using transfer learning and convolutional neural network," Neural Networks, vol. 128, pp. 47–60, 2020.

[21] J. Folmsbee, X. Liu, M. Brandwein-Weber, and D. Scott, "Active deep learning: improved training efficiency of convolutional neural networks for tissue classification in oral cavity cancer," in Proceedings of the IEEE 15th International Symposium on Biomedical Imaging (ISBI 2018), pp. 770–773, Washington, DC, USA, April 2018.

[22] F. Martino, D. D. Bloisi, A. Pennisi et al., "Deep learningbased pixel-wise lesion segmentation on oral squamous cell carcinoma images," Applied Sciences, vol. 10, no. 22, 2020.

[23] I. Amin, H. Zamir, and F. F. Khan, "Histopathological image analysis for oral squamous cell carcinoma classification using concatenated deep learning models," medRxiv, http:// medrxiv.org/content/early/2021/05/14/ 2021.05.06.21256741. abstract, 2021

[26] Chu, C.S., Lee, N.P., Adeoye, J., Thomson, P. and Choi, S.W., 2020. Machine learning and treatment outcome prediction for oral cancer. *Journal of Oral Pathology & Medicine*, *49*(10), pp.977-985.

[27] Welikala, R.A., Remagnino, P., Lim, J.H., Chan, C.S., Rajendran, S., Kallarakkal, T.G., Zain, R.B., Jayasinghe, R.D., Rimal, J., Kerr, A.R. and Amtha, R., 2020. Automated detection and classification of oral lesions using deep learning for early detection of oral cancer. *IEEE Access*, *8*, pp.132677-132693.

[28] Alhazmi, A., Alhazmi, Y., Makrami, A., Masmali, A., Salawi, N., Masmali, K. and Patil, S., 2021. Application of artificial intelligence and machine learning for prediction of oral cancer risk. *Journal of Oral Pathology & Medicine*, *50*(5), pp.444-450.

[29] Rahman, T.Y., Mahanta, L.B., Das, A.K. and Sarma, J.D., 2020. Histopathological imaging database for oral cancer analysis. *Data in brief*, *29*, p.105114.